 https://doi.org/10.3011/ESARDA.IJNSNP.2020.9

A methodology to identify partial defects in spent nuclear fuel using gamma spectroscopy data

Zsolt Elter, Sophie Grape

Uppsala University
Department of Physics and Astronomy, Division of Applied Nuclear Physics
Ångströmlaboratoriet, Lägerhyddsvägen 1
E-mail: zsolt.elter@physics.uu.se, sophie.grape@physics.uu.se

Abstract:

This paper describes a methodology to identify partial defects in modelled spent nuclear fuel using passive gamma spectroscopy data. A fuel library, developed with Serpent2, was used to calculate the material composition of spent nuclear fuel. Two fuel configurations were investigated in this work; one where the fuel assembly configuration was intact and one where 30% of the fuel rods were substituted with stainless steel rods in a random configuration. Emission and detection of gamma radiation from ^{134}Cs, ^{137}Cs and ^{154}Eu was simulated using a model of a passive gamma spectroscopy measurement station mimicking the Clab measurement station in Sweden. A simple HPGe detector model was implemented, and its detector efficiency was assessed using a range of different source energies. Realistic total gamma attenuation coefficients were calculated using the XCOM database. The modelled estimates of detected full-energy peak counts were then used in a Principal Component Analysis in order to investigate whether it was possible to distinguish between intact and partial defect fuel assemblies or not. The results showed that partial defects could be identified using the simultaneous analysis of all three peak intensities, and that the ability to do so increased when only gamma emission energies from ^{154}Eu were considered.

Keywords: safeguards; partial defect; PCA; nuclear fuel; multivariate analysis;

1. Nuclear safeguards and the verification of spent nuclear fuel

1.1 Verification of spent nuclear fuel using the existing safeguards framework

Under the Non-Proliferation Treaty [1], nuclear material needs to be safeguarded to ensure that it is not being diverted and used for non-peaceful applications. For this reason, spent nuclear fuel is regularly verified by nuclear safeguards inspectors. The inspectors are able to perform non-destructive assay (NDA) measurements on the fuel, in order to draw conclusions on the completeness and correctness of declarations. This is especially important before placing the fuel in so-called difficult-to-access storage where re-verification is not possible.

During the past decade, efforts have been ongoing to increase the capability to detect so-called partial defects in spent nuclear fuel, whereby a fraction of the nuclear material has been diverted or substituted. The efforts concern investigations of partial defect detection capability in mainly two different categories of nuclear safeguards instrumentation: i) instrumentation currently used in safeguards inspections, such as the Fork detector [2-4]) or the Digital Cherenkov Viewing Device (DCVD) [5]) and ii) instrumentation under development, or recently developed, for enhanced safeguards assessments such as partial defect detection [6,7]. In addition to these two categories, there are general detection techniques that could be investigated for enhanced safeguards performance and partial defect detection capability, such as passive gamma spectroscopy, which is the topic of this work. Earlier safeguards studies have shown the relevance of this technique [8,9].

The current partial defect detection level for spent nuclear fuel is on 50% of the fuel rods, but with the recent introduction of the passive gamma-emission tomography instrument denoted PGET, it is believed that verification of partial defect level on the single rod level will be possible [7]. However, it has also been shown [10] that if a sampling plan is to be developed for the verification procedure, it would be advantageous to also have additional instruments with partial defect detection capability at levels somewhere between the 50% level and the single pin level. High-resolution gamma spectroscopy is a measurement technique that can be envisaged for this purpose, since some facilities already have the equipment in place and is already used to verify operational parameters such as burnup (e.g. ASEA-ATOM facilities such as all the Swedish nuclear power plants and Clab [11]), whereas others could plan for such equipment when planning for or constructing new facilities (such as the planned encapsulation facility Clink in Sweden).

1.2 This work

It has been reported over the past years that there is a need for efficient and cost-effective safeguards verifications from the International Atomic Energy Agency (IAEA), and the use of machine learning tools and artificial intelligence in nuclear

 Elter, Z., & Grape, S. (2020). A methodology to identify partial defects in spent nuclear fuel using gamma spectroscopy data. *ESARDA Bulletin - The International Journal of Nuclear Safeguards and Non-proliferation*, 61, 22-31. https://doi.org/10.3011/ESARDA.IJNSNP.2020.9

safeguards is being investigated for different purposes [12-14]. Accordingly, investigating ways to make optimal use of data that has already been, or can be, collected using automatic machine learning tools is of high priority.

Against this background, this work presents a methodology that can be used to investigate whether or not partial defects can be identified in spent nuclear fuel assemblies, using a modelled passive gamma spectroscopy response and differences in gamma attenuation. The software that has been developed for geometric efficiency calculations is already publicly available [15] and the scripts that have been written for this specific work are available on GitHub [16]. The choices made by the authors in this work considering the measurement station, the gamma detector (type, geometry and design) as well as the spent nuclear fuel itself can be defined and changed by the user. For that reason, the results of the analysis here should merely be seen as an example of what information that can be obtained using this methodology, given the choices made by the user.

2. Spent nuclear fuel handling in Sweden

Sweden currently has six nuclear power plants (NPPs) in operation. After discharge from the reactor, the fuel is cooled in a fuel pond at the reactor site for around 1 year before it is shipped to Clab. SKB, the company that owns Clab, handed in an application to construct and operate a final repository for spent nuclear fuel in 2011. So-far, the Swedish government has still not taken a stand on the issue. According to the plans, the fuel to be encapsulated will cover a variety of fuel types (where BWR and PWR fuels are by far the most common types), fuel designs and fuel parameters [17]. The fuel assemblies are expected to have cooling times of up to around 70 years, while burnups are expected to reach up to around 60 MWd/kgHM. Before encapsulation, which will take place in the future Clink facility, the fuel assemblies will reside in water ponds in Clab where they are stored underground, in baskets holding up to 25 fuel assemblies at a time (25 BWR fuel assemblies or 16 PWR fuel assemblies).

Fuel handling equipment exists both at the NPPs and at Clab, but there are essential differences. At the reactor sites, the equipment is constructed to be able to handle manipulation of complete fuel assemblies for loading/unloading into the reactor, but also individual fuel rods in case of fuel damage when a single fuel rod needs to be removed/replaced. Clab has no equipment to handle individual fuel rods at all, and can only handle fuel assemblies in the reception area. At Clab, fuel assemblies are placed in baskets holding multiple fuel assemblies, before they are transported to the underground pools. The fuel handling machine in the underground pool area can only handle baskets. Partial defect verification is primarily of interest before transporting spent nuclear fuel to difficult-to-access storage, which means that such verification will most likely be done in the Clink facility, and neither at the NPPs nor in Clab. What fuel handling equipment or fuel assay instrumentation that will be available in Clink is not yet determined but it seems probable that only fuel elements (and not single fuel rods) will be handled. Based on this information, it appears that the only facilities currently equipped to pull and replace fuel rods are the NPPs, whereas verification of such defects is mainly planned take place in connection to verification before placement in difficult-to-access storage sites, long after such defects may be caused i.e. on long-cooled spent nuclear fuel, unless there are specific reasons to require this type of verification at an earlier stage such as a lost Continuity of Knowledge.

Hence, analysing remaining fission products with relatively long half-lives to possibly identify partial defects make sense, or one should recommend that partial defect verification is performed much earlier.

3. Methodology to calculate and analyze the number of counts in full-energy peaks

This section aims at describing the proposed methodology in different steps.

3.1 Overview of the methodology

A measure of the number of counts in the full-energy peak at a certain energy line in a gamma spectrum can be calculated by

$$f(E) = I_\gamma(E)\cdot\varepsilon_g(E)\cdot\varepsilon_d(E) = I_\gamma(E)\cdot\varepsilon_p(E) \quad (1)$$

where $I_\gamma(E)$ is the emission frequency of a certain energy line, $\varepsilon_g(E)$ is the energy-dependent geometric efficiency which describes the probability of a particle arriving at the detector from the source, and $\varepsilon_d(E)$ is the energy-dependent intrinsic detector efficiency which describes the probability of a particle leaving its full energy inside the detector. The multiplication of the last two efficiency functions can be defined as the full-energy peak efficiency $\varepsilon_p(E)$ of the setup. In gamma spectroscopy measurements of spent nuclear fuel, the emission frequencies $I_\gamma(E)$ depend on the nuclide inventory of the fuel assembly, and thus on its operational history and the amount of radioactive material in the assembly. Thus $I_\gamma(E)$ will be affected by a partial defect, but cannot in itself provide conclusive evidence of a defect. The geometric efficiency $\varepsilon_g(E)$ depends on the experimental setup (i.e. how far away the detector is placed from the source and what kind of absorbing material that is placed between them), the geometry of the fuel assembly, and as it will be shown later, the operational history through the change of the total gamma attenuation coefficient of the fuel. Finally, the detector efficiency $\varepsilon_d(E)$ depends on the geometry of the detector. Therefore, in a given setup (where the location of

the detector and the assembly is fixed), the change in the geometric efficiency should provide evidence of the defect.

In order to calculate the number of counts in different full-energy peaks for a given burnup (BU), cooling time (CT), initial enrichment (IE), the three functions in Eq. (1) have been tackled separately. An overview of the proposed methodology is shown in Figure 1, and the different steps are described in detail in the following subsections. A supplementary jupyter notebook and related python module can be found at [16] to demonstrate how the steps can be performed in practice.

In this work, a partial defect level of 30% has been considered because it constitutes an intermediate level to the detection capabilities of other safeguards instruments available today. 80 fuel rods were thus substituted against stainless steel rods in one random configuration, shown in Step 2 of Figure 1, where the pink fuel rods mark the steel dummy rods. The remaining low-enriched uranium fuel rods have the same material composition as those in the corresponding intact fuel assembly. The selected partial defect level and substitution material can be chosen differently, but the investigation of other configurations is outside the scope of this work and will be targeted in future research.

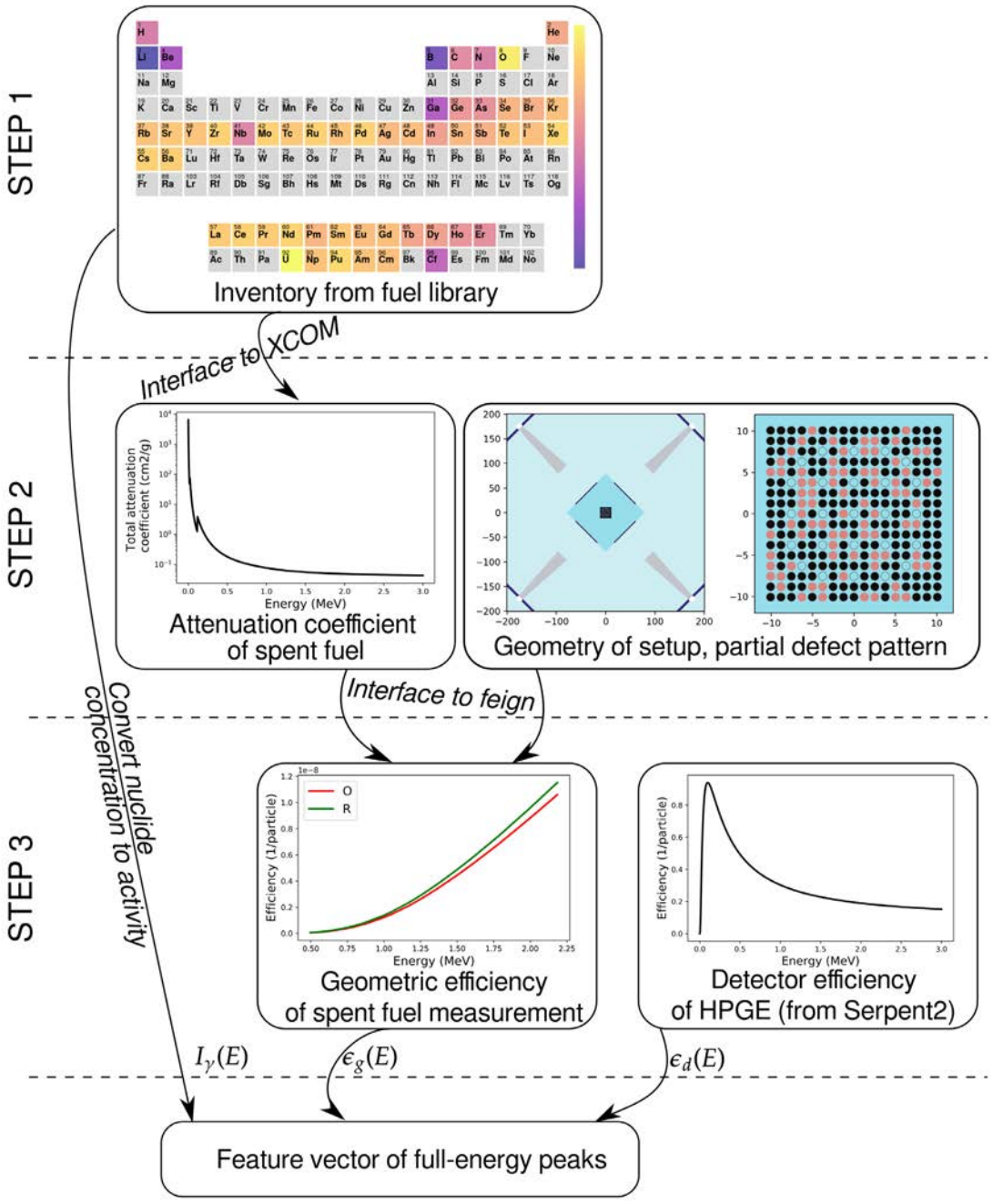

Figure 1. Summary of the proposed methodology

3.2 Step 1 - Determining the spent fuel nuclide inventory

The spent fuel nuclide inventories were sampled from an already existing PWR spent fuel library. The samples in the library were created by performing depletion calculations in a pin cell model with the Serpent2 code [18]. Further details on the fuel library and how it was created can be found in [19]. The fuel library itself is available at [20].

For the current study, 200 spent UO_2 fuel samples with a BU of 20-70 MWd/kgU and CT less than 30 years were randomly selected. Their respective concentrations of various isotopic concentrations were then extracted. As ^{134}Cs, ^{137}Cs and ^{154}Eu contribute significantly to the gamma spectrum at the cooling times considered in this work, only the gamma lines summarized in Table 1 were included. However, the supplemented python code can be extended with additional nuclides and associated energy lines without difficulty. The nuclide concentrations C_n were converted into gamma-line emission activities $A_{n,l}$ according to

$$A_{n,l} = C_n \cdot \frac{ln(2)}{T_{1/2,n}} I_{n,l} \tag{2}$$

where the half-lives of the nuclides $T_{1/2,n}$ and the intensities of the energy lines $I_{n,l}$ are given in Table 1. One has to note here that in order to obtain the actual number of counts in a detector, these per-volume quantities need to be multiplied by the spent nuclear fuel volume contributing to the detector signal. However, as detailed later, in this work only the values per fuel volume were used (no absolute values).

Nuclide	Half-life (y)	γ-lines (MeV)	Intensities (%)
^{134}Cs	2.065	0.563, 0.569, 0.604, 0.795, 0.801, 1.038, 1.167, 1.365	8.338, 15.373, 97.62, 85.46, 8.688, 0.990, 1.790, 3.017
^{137}Cs	30.1	0.662	85.1
^{154}Eu	8.6	0.723, 0.756, 0.873, 0.996, 1.004, 1.246, 1.274, 1.494, 1.596	20.06, 4.52, 12.08, 10.48, 18.01, 0.856, 34.8, 0.698, 1.797

Table 1: The gamma-ray emitting nuclides and their gamma-lines considered in this study.

3.3 Step 2 - Obtaining the accurate total gamma attenuation coefficients

Fresh light water reactor nuclear fuel consists of a mixture of uranium and oxygen, whereas spent nuclear fuel also contains a plethora of lighter fission products and heavier actinides. The difference in material composition as a function of BU impacts the attenuation of gamma rays, and was recently shown to be non-negligible in gamma spectrometry applications [21]. In order to accurately take into account and assess the impact of the change in the attenuating properties of spent nuclear fuel, we have created an interface between the nuclide inventory data and the XCOM software which calculates total attenuation cross-sections of materials [22]. Step 2 of Figure 1 includes an example of the total attenuation coefficient calculated for a spent fuel inventory.

3.4 Step 3 - Determining the full-energy peak efficiency

As pointed out previously, the full energy peak efficiency is determined by considering the geometric efficiency of the measurement setup and the detector efficiency separately.

3.4.1 Geometric efficiency of the modelled setup

In this work, the actual dimensions of the experimental setup are not important per se, but used as an example to show how the methodology can be used for any arbitrary measurement setup. Nevertheless, the dimensions of the passive gamma spectroscopy station at Clab were adopted. At Clab, the spent fuel is placed in a fixture mounted on the pool wall with a ~50 cm distance between the center of the assembly and the pool wall. The fixture is able to rotate the fuel assembly and also move it in axial direction. In the 2m thick concrete pool wall, there is an air-filled hole, partially filled with a steel collimator. The steel collimator is made of two massive steel half cylinders, covered with a steel window. The height of the collimator slit can be adjusted in the range of 1-3 mm to allow for different counting rates in the detector. The length of the steel collimator is 1.2 m, and the distance from the center of the fuel assembly to the end of the collimator is 2.46 m. In the model, between the end of the collimator and the detector, 4 absorber sheets are placed (8 mm of lead, 3 mm of aluminium, 21 mm of steel and 1 mm of copper) in order to filter out low-energy gamma rays. The setup is described in greater detail in [23, 24].

The geometric efficiency of this measurement station was computed with the feign package [15] which implements a 2D ray-tracing method without build-up factors. The package allows the user to define a rectangular fuel assembly, a pool around it, various absorbers and detector points with their associated collimators. A radial view of the geometry of the setup is shown in Step 2 of Figure 1. The geometric efficiency of the setup has been averaged over four detector locations, with each location facing one of the fuel assembly corners, thereby mimicking the rotation of the fuel assembly around the vertical axis in real-life measurements. This averaging plays a role in case the fuel assembly is asymmetric.

In the current work, the geometric efficiency was evaluated for the two cases of an intact 17x17 PWR assembly (noted as “O” for original), and a 30% partial defect 17x17 fuel assembly (later noted as “R” for random). The difference in geometric efficiency curves (as shown in Step 3 in Figure 1) demonstrates how manipulation of the fuel assembly may be identified.

3.4.2 Detector efficiency

A simple HPGe geometry with a crystal diameter and length of 60.5 mm and 61 mm was simulated. The core hole diameter and depth were 12 and 51 mm, respectively. Serpent2 simulations were made with a pen-beam source placed 1 cm above the central axis of the detector crystal for several source energies. A damped exponential function was fitted to the detector response to describe the detector efficiency curve, as shown in Step 3 of Figure 1. For fitting the function

$$ln\left(\epsilon_d\right) = a + b \cdot ln\left(\frac{E}{f}\right) + c \cdot ln^2\left(\frac{E}{f}\right) + d \cdot ln^3\left(\frac{E}{f}\right) + e \cdot ln^4\left(\frac{E}{f}\right) \quad (3)$$

was used, as proposed also in [25]. The fitting and the values of the parameters are available in the supplemented notebooks.

3.5 Creating the feature matrix and PCA

The previous sections summarized how each of the functions of Eq. (1) can be estimated. The following step is to multiply the functions for each considered gamma-ray energy emitted by the given spent fuel. Finally, each fuel sample can then be represented by a multi-dimensional feature vector, with each feature vector corresponding to the full-energy peak counts for all isotopes as described by Eq. (4). The sum of the feature vector was normalized to 1 as shown in Eq. (5), in order to give all features f_i (despite possible differences in magnitude) the same importance in the multivariate analysis (in the current case typically the 137Cs peak would have such an impact).

$$\underline{f} = \begin{pmatrix} f\left(E_{^{137}Cs_{0.662}}\right), f\left(E_{^{134}Cs_{0.563}}\right), \ldots, \\ f\left(E_{^{154}Eu_{0.723}}\right), \ldots, f\left(E_{^{154}Eu_{1.596}}\right) \end{pmatrix} \quad (4)$$

$$\underline{f}_{norm} = \frac{\underline{f}}{\sum_i f_i} \quad (5)$$

Since 200 nuclide inventories were used and the geometric efficiency was calculated for both intact and manipulated fuel, the analysis includes 400 feature vectors, which can be arranged into a feature matrix. In the feature matrix, each row corresponds to the feature vector of a specific spent nuclear fuel sample, and each column corresponds to the full-energy peak counts for a certain gamma-ray energy. The matrix underwent standard scaling meaning that for each column the mean is centered to 0 and the variance is renormalized to 1. The feature matrix is often referred to as a predictor matrix, since it is used to predict targets or responses which can be assigned to each sample. Such a response could be for example the reactor type for classification problems, or the fuel parameters BU and CT for regression problems. In this work, the response was whether or not the fuel assembly was intact. Through a simple encoding, the label “0” was assigned to samples of intact fuel, and the label “1” to all other samples, and all responses were collected in the so-called response vector.

A feature ranking was performed on the data matrix to investigate the importance of the different gamma-ray energies in the classification of the fuels, based on the so-called Pearson’s correlation score between the energies and the responses. The correlation score defined as

$$corr\left(x_i, y\right) = \frac{E\left(x_i \cdot y\right) - E\left(x_i\right) \cdot E\left(y\right)}{\sigma_{x_i} \cdot \sigma_y} \cdot 100(\%) \quad (6)$$

was used to rank the features according to their importance. Here x_i can be a column of the feature matrix, or a vector derived from several columns (eg. the ratio of two peaks).

Since the data is multidimensional (18 full-energy peak counts), it is difficult to visualize. A widely used dimensionality reduction technique called Principal Component Analysis (PCA) [26,27] was applied to investigate patterns within the data set, and analyze whether intact cases could be distinguished as such. PCA uses an orthogonal transformation to convert the original set of possibly correlated features (eg. multiple full-energy peak counts from the same isotope are necessarily strongly correlated) into a set of linearly uncorrelated variables. These variables are called Principal Components (PCs). The number of PCs is less than or equal to the original dimension of the feature vector. In the current study, the Scikit-learn python library [28] was used to perform the PCA.

3.6 Approximations and assumptions made in the analysis

In the analysis, many simplifying assumptions have been made:

- There has been no attempt to estimate an absolute number of counts in any of the selected full energy peaks, only an estimate of the number of counts per source volume and unit time. Due to this, certain effects were neglected such as an estimate of the fraction of the fuel assembly seen by the detector. This is in turn related to the exact dimensions of the collimator slit, which is 8.5 cm wide and variable in height. In an estimation of the absolute number of counts in a detector, a surface source with an angular distribution is a better approximation than the pen-beam source model used in the detector efficiency simulations here.

- No measurement noise is included in the analysis, but it is also not considered to be of major importance to this work since there are no attempts made to estimate an absolute number of counts. However, various (constant) background levels could impact the capability to correctly determine peak areas to use in the analysis, and hence such effects should be looked closer upon in future work, as absolute count rates are also taken into account.
- Since the absolute number of counts is not of interest, there has been no need to look into aspects concerning calibration issues of the detector setup.
- The electronic equipment needed for the gamma spectroscopy measurements has not been considered or modelled.
- There has been no attempt to actually train a classifier algorithm nor to estimate uncertainties in the results from considering different partial defect patterns, substitution materials or uncertainties in the operator-declared values IE, BU or CT. Also, only a standard irradiation cycle has been considered in the depletion calculations.
- Although the change in the attenuation coefficient of the spent fuel due to BU was taken into account, the change in the density and rod radius due to swelling was not considered. Also all rods within the same spent fuel assembly were considered to have identical burnup and inventory.

One could imagine to consider multiple approximations using some constant shape factor. If doing so, the constant would disappear in the normalization of the feature matrix, and thus in a noise-free (i.e. infinitely long) measurement it would have no impact.

4. Results and discussions

4.1 Feature ranking

The correlation between the features and the response vector were evaluated according to Eq. (6) and the correlation scores are given in Table 2. The ^{154}Eu lines have the highest correlation score to the identification of partial defects in the fuel, and the higher the gamma-ray energy is the higher the correlation score is. One can see that the correlation scores are lower than 10% for each feature, which indicates that peak counts from one single gamma-ray energy does not carry much information on whether the fuel is intact or not. The low correlation scores are expected, since replacing fuel rods will impact the probability of low and high energy photons reaching the detector differently. For example, low-energy photons reaching the detector originate most probably from the peripheral rods, since the central rods are shielded. Thus, replacing the peripheral fuel rods will have a larger impact on the low-energy range of the geometric efficiency than on the high-energy range. Accordingly, including multiple peaks in the analysis should correlate more to the response vector.

Nuclide, γ-line (MeV)	Corr. Score (%)	Nuclide, γ-line (MeV)	Corr. Score (%)
^{154}Eu, 1.596	9.55	^{134}Cs, 0.563	1.44
^{154}Eu, 1.494	9.21	^{134}Cs, 0.569	1.39
^{154}Eu, 1.274	7.95	^{134}Cs, 1.038	1.37
^{154}Eu, 1.246	7.73	^{134}Cs, 0.604	1.10
^{154}Eu, 1.004	4.99	^{137}Cs, 0.662	0.85
^{154}Eu, 0.996	4.88	^{154}Eu, 0.756	0.62
^{154}Eu, 0.873	2.92	^{134}Cs, 0.801	0.24
^{134}Cs, 1.365	2.28	^{134}Cs, 0.795	0.21
^{134}Cs, 1.167	1.81	^{154}Eu, 0.723	0.12

Table 2: Correlation scores of normalized peaks to class

One way to include multiple gamma-ray energies in the feature ranking is to calculate peak ratios for all possible combinations of the 18 gamma-ray energies. This was done here and the correlation scores were then re-calculated for the ratios and the response vector. In this case, the feature matrix was not standard scaled, since the scaling would obscure any correlations. The number of correlation scores are more than a hundred, and not easily shown in a table, but it is worth pointing out that the correlation scores dramatically increased. The highest correlation score, 99.34%, was obtained for the ratio of the 1.494 MeV and 1.246 MeV peaks of ^{154}Eu. In general, the ratios involving the different ^{154}Eu and ^{134}Cs gamma-ray energies resulted in very high correlation scores (over 90%), whereas correlation scores in which ^{137}Cs was included were below 7%. This shows that ^{137}Cs, having only a single energy line, is not helpful in classifying partial defects based on the changes in the geometric efficiency and that indeed a multivariate approach is needed when verifying partial defects with passive gamma spectroscopy.

4.2 Principal Component Analysis

Using the feature matrix described earlier, a Principal Component Analysis (PCA) was performed. Figure 2 illustrates the first three Principal Components (PCs), i.e. the three PCs that account for the largest variance in the data when all the 18 gamma lines from Table 1 are included in the matrix. One can observe that the two cases, “O” and “R”, are well-separated in the three-dimensional space spanned by the three first PCs. However, it can be also noticed that only the third PC bears any information on the identification of partial defects. Further investigations show that the variability in the first two PCs is caused by the so-called nuisance parameters BU and CT i.e. parameters which are not of direct interest but that must be taken into account in the analysis. Figure 2, displaying the two parabola-shaped clusters of data points, illustrates that the first two PCs are dominated by the CT-dependence of the fuel samples. The longer the cooling time is, the less pronounced the separation between the two cases is.

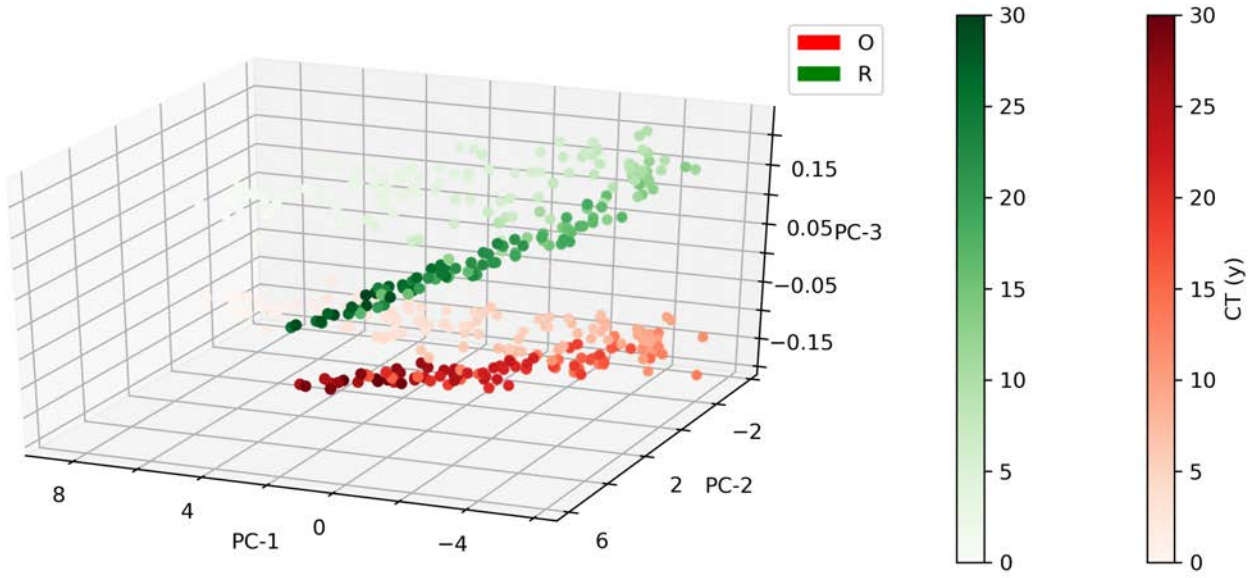

Figure 2: Principal Components of the dataset with all ^{134}Cs,^{137} Cs and ^{154}Eu peaks included.

There are several options available to suppress the importance of BU and CT in the data. Two options are to correct for the CT if that information is available (in practice often that is a value to be verified), or to use ratios of counts in different full-energy peaks. Here, an even more straightforward approach was used: the feature ranking implied that the ^{154}Eu lines carry the most relevant information when classifying fuel samples and thus only information on those gamma-ray energies were kept in the feature matrix. Since the ^{154}Eu concentration in the spent nuclear fuel is the same no matter what ^{154}Eu gamma-ray energy that is analyzed, one can expect that the impact of BU and CT becomes suppressed in the PCs. This can in fact be seen in Figure 3, which also shows the impact of using the actual total gamma attenuation coefficient. The left panel of Figure 3 shows the first two PCs for the case when the total gamma attenuation coefficient from XCOM was taken into account for each fuel sample. One can observe that now already the first PC provides information on the presence of partial defects, and that the spread in mainly the direction of PC-2 is due to the variation of BU (and hence attenuation) among the fuel samples. In the right panel of Figure 3, the first two PCs are illustrated for the case when the total gamma attenuation coefficient corresponding to fresh fuel was used for each sample. It is seen that this simplifying assumption leads to the removal of any BU and CT dependencies in the data, and that all the fuel samples end up at the exact same place on the PC coordinate system. Apparently, the impact of nuisance parameters has been successfully eliminated. It is also clearly seen that it is sufficient to only consider the first PC in order to correctly identify partial defects in the spent nuclear fuel assemblies in this case. However, the difference between the right and left panels show that the impact of the change in the attenuation coefficient is not negligible. Thus, in a practical case when the presence of partial defect (on any level) is to be predicted based on a measured gamma spectrum, the predictor model needs to be trained with data which accounts for that.

5. Conclusions

The current paper described a fast, robust and flexible methodology to estimate and analyze full-energy peak counts in passive gamma spectroscopy measurements of spent nuclear fuel. The methodology evaluates the modelled counts-per-volume and time in a simple HPGe detector, by separately taking into account the activity of different gamma-emitting nuclides in the spent fuel, estimating the geometric efficiency of the measurement setup and simulating the intrinsic detector efficiency of an HPGe detector. The methodology is flexible in the manner that the user may define a different measurement setup or detector design to study.

An application of this methodology was shown here. The purpose was to investigate the possibility of identifying partial defects in spent nuclear fuel. The modelled fuel was intact 17x17 PWR fuel assemblies and manipulated 17x17 PWR fuel assemblies, suffering from a 30% partial defect level. It was shown that the geometric efficiency did in fact depend on the presence of the partial defect, due to the different attenuation of low and high-energy gamma-rays by the fuel assembly itself. For 200 spent nuclear fuel samples, the per-volume and unit time counts in the full-energy gamma peaks of ^{134}Cs, ^{137}Cs and ^{154}Eu were estimated

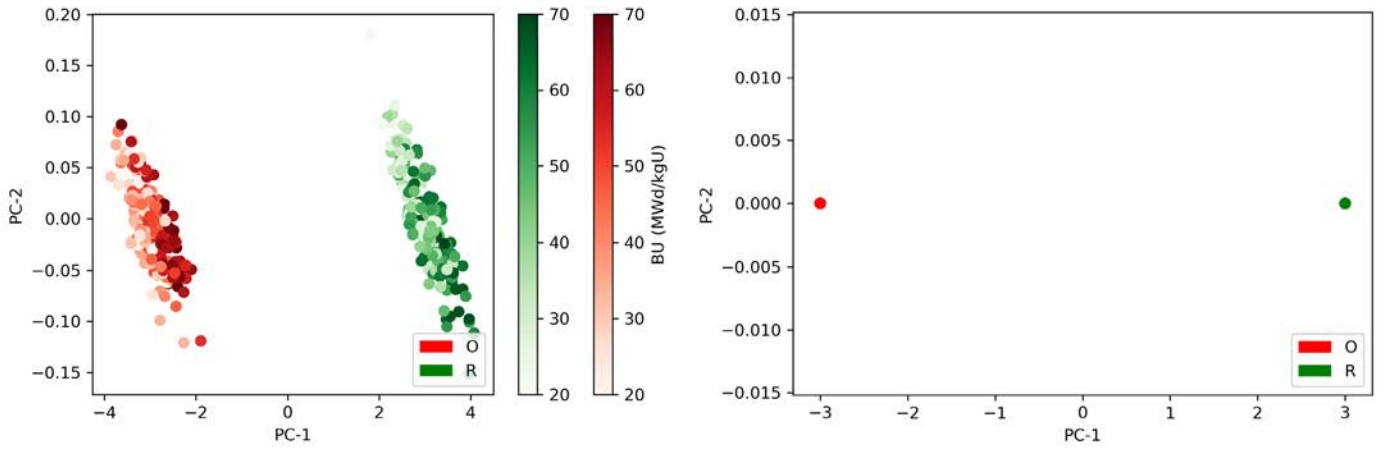

Figure 3: Principal Components of the dataset including only ^{154}Eu peaks. Left: Inventory-dependent attenuation coefficients from the XCOM database are used. Right: The attenuation coefficient of fresh UO_2 fuel is used for all samples.

and analysed with PCA. It was shown that just by using the peak counts-per-volume and time without any calibration, one can distinguish intact and manipulated fuel, however the BU and CT parameters act as nuisance parameters and need to be accounted for. As a solution found here was to only include the ^{154}Eu lines in the analysis. It was also shown in the analysis that considering a more realistic total gamma attenuation coefficient rather than a simplified fixed value, impacts the per volume and time counts in the detector and thus also the classification to some extent.

The possible draw-back identified with the use of only Eu-154 is its relatively short half-life of 8.6 years. In the verification of spent nuclear fuel before encapsulation, it is likely that many fuel assemblies will have a very long CT and thus there will be little Eu-154 left to detect. A solution to this could be to perform the partial defect verification earlier, for instance in connection to receiving the fuel at Clab, or even before shipping it to Clab from the NPP sites. The fact that the receiving facility does not have capability to manipulate spent nuclear fuel on the single rod level, in combination with Containment and Surveillance measures and other tools available to ensure that Continuity of Knowledge is kept, could possibly enable partial defects to be reliably detected.

6. Outlook

Since this paper mainly focused on the methodology and on giving a proof-of-principle, it was not intended to cover a large set of various partial defect scenarios. Nevertheless, we have begun the continuation of this work in which the methodology is used to investigate a large number of different partial defect patterns as well as different partial defect levels and different substitution materials.

Also, as the continuation of this work we would like to investigate how robust the methodology is to measurement noise. For this we will need to estimate the absolute value of the peak counts. In order to achieve that we are currently extending the software feign to handle 3D effects such as the impact of the fan-shaped view-angle of the collimator, and we are also going to improve the detector efficiency simulations to take into account a more realistic surface source.

Finally, it has to be noted that performing the PCA provided only an opportunity to visualize whether intact and manipulated fuel could be identified, although a proper classification method has not been developed. The next step will be to train classification methods, such as for instance artificial neural networks, and assess how well intact fuel can be discriminated from manipulated fuel in the presence of noise and to get an indication of the lowest level of partial defects that can be reliably detected with passive gamma spectroscopy.

7. Acknowledgements

We would like to acknowledge the Swedish Radiation Safety Authority for supporting this work under contracts SSM2017-5979 and SSM2020-996. We would also like to thank Carl Hellesen for the helpful discussions in the early stages of this work. Special thanks to Peter Andersson and Lorenzo Senis for the discussions regarding the simulation of the response function in a passive gamma measurement setup.

Finally, we would like to acknowledge that the coloured periodic table in Figure 1 was created with the python module created by Andrew S. Rosen [29].

8. References

[1] International Atomic Energy Agency (IAEA), *Treaty on the non-proliferation of nuclear weapons*. INFCIRC/140., (1970)

[2] Tiita, A., Saarinen, J., Tarvainen, M., Axell, K., *Investigation on the possibility to use fork detector for partial defect verification of spent lwr fuel assemblies: Final report on Task JNT A 1071 (BEL, FIN, SWE) of the Member States' Support Programme to IAEA Safeguards*. STUK report series, ISSN 0785-9325 ; STUK-YTO-TR 191 (2002)

[3] Meer, K. van der, Coeck, M., *Is the FORK detector a partial defect tester?* Symposium on international safeguards: Addressing verification challenges; Vienna (Austria); IAEA-CN--148/68 (2006)

[4] Rossa R., Borella A., Giani N., *Comparison of machine learning models for the detection of partial defects in spent nuclear fuel*. Annals of Nuclear Energy, Volume 147, (2020)

[5] Branger E., *Enhancing the performance of the Digital Cherenkov Viewing Device: Detecting partial defects in irradiated nuclear fuel assemblies using Cherenkov light*. Doctoral thesis, Uppsala University. ISSN 1651-6214 (2018)

[6] Tobin S.J., et al.. *Quantifying the plutonium mass in spent fuel assemblies with nondestructive assay – an update on the NGSI research effort*. In: Proceedings of the 52nd INMM annual meeting (2011)

[7] Jacobsson Svärd S. et al.; *Tomographic determination of spent fuel assembly pinwise burnup and cooling time for detection of anomalies*, 37th annual ESARDA Symposium

[8] Hellesen C., Grape S., Jansson P., Jacobsson Svärd S., Åberg Lindell M., Andersson P., *Nuclear Spent Fuel Parameter Determination using Multivariate Analysis of Fission Product Gamma Spectra*, Annals of Nuclear Energy, Volume 110, Pages 886-895 (2017)

[9] Elter Zs., Caldeira Balkeståhl L., Grape S., Hellesen C. Partial defect identification in PWR spent fuel using Passive Gamma Spectroscopy, Physor 2018 conference proceedings (2018)

[10] Hellesen C., Grape S., *Non-destructive assay sampling of nuclear fuel before encapsulation*, ESARDA Bulletin No 56, (2018)

[11] *Private communication*, Prof. Ane Håkansson, Uppsala University (2020)

[12] Rockwood L., Mayhew N., Lazarev A., Pfneisl M., *IAEA Safeguards: Staying Ahead of the Game*, Report by the Swedish Radiation Safety Authority, Report number: 2019:14 ISSN: 2000-0456 (2019)

[13] Shoman N., Cipiti B. B., *Unsupervised Machine Learning for Nuclear Safeguards*, Annual Meeting Proceedings of Institute of Nuclear Materials Management, July 22-26, 2018 in Baltimore, Maryland (2018)

[14] Haddal R., Hayden N., *Autonomous systems, artificial intelligence and safeguards*, IAEA Symposium on International Safeguards Building Future Safeguards Capabilities, (2018)

[15] Elter Zs., Cserkaszky A., Grape S., *feign: a Python package to estimate geometric efficiency in passive gamma spectroscopy measurements of nuclear fuel*, The Journal of Open Source Software 4(42):1650 (2019)

[16] Elter Zs. A methodology to identify partial defects in spent nuclear fuel using gamma spectroscopy data (supplementary software) (Version v1.0) Zenodo. http://doi.org/10.5281/zenodo.4250073 (2020)

[17] Svensk Kärnbränslehantering AB, *Spent nuclear fuel for disposal in the KBS-3 repository*, Technical Report TR-10-13 (2010)

[18] Leppänen J. et al., The Serpent Monte Carlo code: Status, development and applications in 2013, Annals of Nuclear Energy 82 pp. 142-150. (2015)

[19] Elter Zs., Pöder Balkeståhl L., Branger E., Grape S., Pressurized water reactor spent nuclear fuel data library produced with the Serpent2 code, Data-in-Brief, Vol 33, DOI: https://doi.org/10.1016/j.dib.2020.106429 (2020)

[20] Elter, Zs., *Uppsala University Pressurized water reactor spent nuclear fuel data library*, Mendeley Data, V1, doi: 10.17632/8z3smmw63p.1 (2020)

[21] Atak H. et al., *The degradation of gamma-ray mass attenuation of UOX and MOX fuel with nuclear burnup*, Progress in Nuclear Energy, Volume 125, (2020)

[22] Berger M.J. et al., *XCOM: Photon Cross Sections Database*, NBSIR 87-3597, DOI: https://dx.doi.org/10.18434/T48G6X (2010)

[23] Vaccaro S. et al., PWR and BWR spent fuel assembly gamma spectra measurements, Nuclear Instruments and Methods in Physics Research Section A: Accelerators, Spectrometers, Detectors and Associated Equipment, Volume 833, Pages 208-225 (2016)

[24] Willman, C, *Applications of Gamma Ray Spectroscopy of Spent Nuclear Fuel for Safeguards and Encapsulation.* Doctoral thesis, Uppsala University. ISSN 1651-6214 (2006)

[25] Mattera, A. *Studying neutron-induced fission at IGISOL-4: From neutron source to yield measurements and model comparisons.* Doctoral thesis, Uppsala University. ISSN 1651-6214 (2017)

[26] Hotelling, H. *Analysis of a complex of statistical variables into principal components.* Journal of Educational Psychology, 24, 417–441, and 498–520. (1933)

[27] Hotelling, H. *Relations between two sets of variates* Biometrika. 28 (3/4): 321–377. (1936)

[28] Pedregosa F. et al. *Scikit-learn: Machine Learning in Python*, Journal of Machine Learning Research 12, pp. 2825-2830, (2011)

[29] Rosen, A. S., *ptable_trends*, python module DOI: 10.5281/zenodo.1451880 (2018)